

# Footprinting the Sites of Interaction of Antibiotics with Catalytic Group I Intron RNA

Uwe von Ahsen and Harry F. Noller

Aminoglycoside inhibitors of translation have been shown previously to inhibit *in vitro* self-splicing by group I introns. Chemical probing of the phage T4-derived sunY intron shows that neomycin, streptomycin, and related antibiotics protected the N-7 position of G96, a universally conserved guanine in the binding site for the guanosine cofactor in the splicing reaction. The antibiotics also disrupted structural contacts that have been proposed to bring the 5' cleavage site of the intron into proximity to the catalytic core. In contrast, the strictly competitive inhibitors deoxyguanosine and arginine protected only the N-7 position of G96. Parallels between these results and previously observed protection of 16S ribosomal RNA by aminoglycosides raise the possibility that group I intron splicing and transfer RNA selection by ribosomes involve similar RNA structural motifs.

Group I introns are a structurally related class of functional RNA elements that are capable of catalyzing their own excision and exon ligation in a well-characterized two-step process (1). Although these catalytic RNAs encompass a wide variety of specific RNA sequences, they share a common secondary structural core (2) and a common self-splicing pathway. It is believed that the RNA structural elements directly responsible for catalysis are contained within the conserved core. The first step of splicing requires attack on the phosphodiester bond at the 5' splice site by a 3' hydroxyl of the guanosine cofactor that binds to a conserved G-C base pair in helix P7 (3) of the conserved core (4). The 5' splice site must therefore be in close proximity to the cofactor binding site. In the second step, the free 3' hydroxyl of the 5' exon attacks the 3' splice site. It is believed that both steps use the same guanosine binding site, so that the 3' terminal G of the intron, in effect, takes the place of the guanosine cofactor in the second step (4-6).

Competitive inhibition of the self-splicing reaction has been found not only for the guanosine analogs deoxyguanosine and dideoxyguanosine (7), but with the guanidino-containing compounds arginine (8) and streptomycin (9, 10). More recently, it was shown that aminoglycoside antibiotics lacking a guanidino group, including neomycin, kanamycin, and gentamicin, specifically inhibit group I intron splicing with inhibition constants ( $K_i$ 's) in the same (micromolar) range in which they affect translation (11). Kinetic studies show that inhibition is noncompetitive of the mixed type, in which both  $k_{cat}$  and the Michaelis constant ( $K_m$ ) for the splicing reaction are affected (12).

The possibility that antibiotics recognize similar RNA target structures in group I

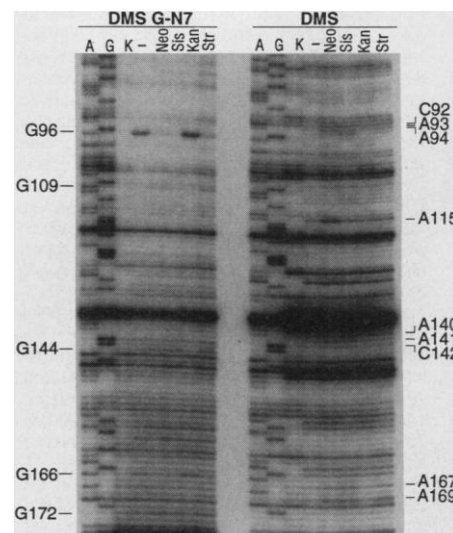
introns and ribosomes (11, 13, 14) led us to search for sites of interaction of antibiotic inhibitors with an abbreviated version (15) of the sunY intron using base-specific chemical probing methods (16). The position and extent of modification are determined by primer extension with reverse transcriptase, which pauses or stops at the modified bases (16, 17). Interactions of antibiotics with the RNA result in perturbations of the reactivity pattern, seen as an increase or decrease in gel band intensities as compared with free RNA. The reactivity pattern of the free RNA (Fig. 1) supports the secondary structure that was deduced for group I intron RNA on the basis of comparative sequence analysis (2) as well as a set of tertiary interactions that have been proposed to play a role in stabilizing the overall folding of the RNA (18). This result, as well as the ability of the RNA to catalyze self-splicing under these conditions (19), show that the intron was in its native conformation during the probing experiments.

Among the very few guanine residues that are attacked at N-7 positions by di-

methylsulfate (DMS) were the strongly reactive G96 (3), which is involved in the conserved G-C pair that is part of the guanosine cofactor binding site in helix P7 (4), and, in order of descending reactivity, G166, G160, and G158 (Fig. 1). Neomycin B, 5-epi-sisomicin, and streptomycin, bound under conditions in which splicing is completely inhibited, all caused complete protection of the N-7 positions of G96 and G166 against methylation by DMS. Base G166 lies in a strongly conserved single-stranded region J8/7, immediately adjacent to the adenine whose N-1 position is involved in an unusual interaction with a 2'-hydroxyl that is located three nucleotides upstream of the 5' splice site (20); this interaction is one of several tertiary contacts believed to position the 5' splice site at the catalytic center. The ability to inhibit the splicing reaction correlates perfectly with the chemical probing results: neomycin, 5-epi-sisomicin, and streptomycin all inhibit splicing, and all three have similar chemical protection and enhancement patterns, whereas the noninhibitory kanamycin A has no detectable effect on the pattern of chemical modification of the RNA, even at concentrations as high as several millimolar. Furthermore, the concentrations of the different antibiotics required for inhibition are similar to those at which their effects on the chemical probing pattern are observed (Fig. 1) (19).

In addition to protection of A43 and A70 in the A-rich J4/5 and J6/6a loops, many drug-induced enhancements were observed, showing that the antibiotics perturb the conformation of the intron RNA (Figs. 1 and 2). No antibiotic-dependent effects were detected in the 3' region of the intron or in the beginning of the 3' exon (19). Neomycin B alone caused a strong enhancement at position A115 and weak protection of A110 and A111 in the L7.1

**Fig. 1.** Probing of the structure of the sunY intron RNA in the presence of antibiotics. SunY precursor RNA (12) was probed with DMS (16) in the presence of 50  $\mu$ M neomycin B, 50  $\mu$ M 5-epi-sisomicin, 50  $\mu$ M kanamycin A, or 500  $\mu$ M streptomycin and was analyzed by primer extension (29). For detection of N-7 positions of guanosine residues, an aniline-induced strand scission was performed (28). Bands corresponding to the bases in the lower left panel were partially obscured by a background of bands between positions 175 and 130 caused by strong spontaneous reverse transcriptase stops that were due to the sodium borohydride-aniline treatment required to detect N-7 methylation (28). Three different primers that hybridize to the 3' exon, stem P9.2, and stem P7 were used to span the sunY intron. A and G, sequencing lanes; K, control (no DMS); -, no antibiotic; Neo, neomycin B; Sis, 5-epi-sisomicin; Kan, kanamycin A; Str, streptomycin.



Sinsheimer Laboratories, University of California at Santa Cruz, Santa Cruz, CA 95064.

loop, indicating either that this antibiotic makes more extensive interactions or that it has an additional binding site on the intron. Finally, in the 5' exon, two bases were weakly protected in the presence of the drugs. Figure 3 summarizes the chemical probing results.

It is not possible to observe directly the interaction of the guanosine cofactor itself with its binding site because its presence in the reaction mixture leads to splicing, which alters the modification pattern. However, we were able to use chemical probing to observe directly the interaction of the cofactor analogs 3'-deoxyguanosine and arginine with the intron. Both inhibitors gave strong protection of the N-7 position of G96 (Fig. 4); we obtained similar results using the inhibitor 2'-deoxygua-

nosine. In contrast to the results found for the antibiotics, no effects were detected elsewhere in the intron or in the surrounding exons. This result provides independent evidence for interaction of these cofactor analogs with the proposed G-binding site (4) and demonstrates for the first time the involvement of the N-7 of G96 in cofactor binding. The N-7 position of G96 of the excised linear sunY intron was protected from DMS attack in the absence of added cofactor (19); this can be explained by binding of the 3' terminal G of the intron to the cofactor binding site (4).

Mutation of the G-C pair at the guanosine cofactor binding site to A-U changes the cofactor specificity from guanosine to 2-aminopurine ribonucleoside (4); however, this mutant intron has the same sensitivity to aminoglycoside antibiotics as the wild-type intron (12). A possible rationale for this is that the N-7 of the adenine could provide an interaction site for the antibiotics in the mutant RNA. To test this possibility, we used another mutant *Tetrahymena* intron in which the base pair at the cofactor binding site contained a G-C to C-G transversion (6). Guanosine or purine ribonucleoside served effectively as cofactors for wild-type or mutant, respectively, giving rise to spliced products (Fig. 5). At 10  $\mu$ M 5-epi-sisomicin, splicing of both introns was strongly inhibited, and at 100  $\mu$ M antibiotic the reaction was completely abolished. Because the mutation dramatically alters the recognition properties of the crucial base pair, we conclude that inhibition of splicing by the antibiotic is independent of the ability of the antibiotic to interact with

the N-7 position of the critical G-C pair in the cofactor binding site.

Among the most prominent effects of the antibiotics on the chemical probing pattern of intron RNA is the virtually complete protection of the strongly reactive N-7 position of G96 in helix P7, a key element of the cofactor binding site (Fig. 1). This same base is the only one protected by the competitive inhibitors deoxyguanosine and arginine, providing direct evidence for the proposed interaction between the guanosine cofactor and the N-7 position of G96 (4). Thus, the competitive component of the inhibitory action of the aminoglycosides can be accounted for by their interaction with the guanosine binding site (21). Because the aminoglycoside inhibitors also cause noncompetitive inhibition (12), it is significant that we found protection of the N-7 position of another strongly conserved guanine, G166, in the single-stranded region connecting stems P8 and P7. Because neither deoxyguanosine nor arginine protect this base, it is unlikely that protection of G166 is due simply to cofactor-

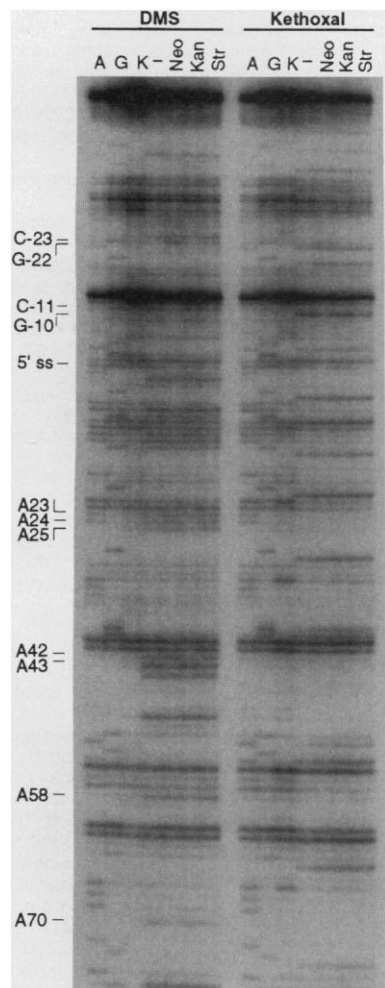


**Fig. 2.** Probing of the 5' region of the sunY intron. Chemical probing conditions were as described in Fig. 1. Kethoxal modification was done as described by Stern *et al.* (16). About 90% of the primer extension products were full-length as opposed to unmodified RNA, indicating less than one methylation per RNA molecule, on average; this minimizes the possibility of structural changes of the RNA caused by multiple methylations; 5' ss, 5' splice site.

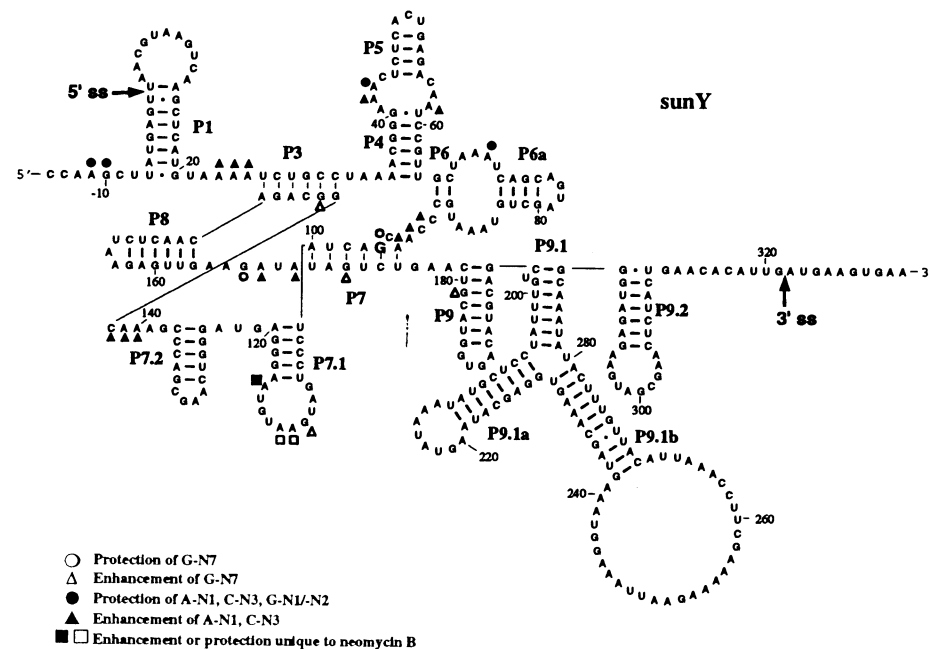


**Fig. 3.** Secondary structure of the sunY intron. Changes in reactivity of bases toward chemical attack in the presence of neomycin B, 5-epi-sisomicin, and streptomycin are indicated.

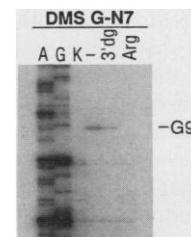


**Fig. 4.** Probing of the interaction of 3'-deoxyguanosine and L-arginine with the sunY intron. Chemical probing, as described in Fig. 1, was performed on ~50 nM sunY precursor RNA in the presence of 5 mM 3'-deoxyguanosine or 50 mM L-arginine (30); 3'dg, 3'-deoxyguanosine; Arg, arginine.

like interaction of the antibiotic with the cofactor binding site. Protection of G166 is therefore the result of additional interactions between antibiotic and RNA. We observed enhanced reactivity for several bases in different regions of the intron that are all believed to interact with the P1 stem (which contains the 5' splice site), giving support to the interpretation that the antibiotics also interfere with interactions between the 5' splice site and the catalytic center. Regions showing enhanced reactivities include J8/7, the site of interaction with the P1 stem (3, 18); the A-rich region J1/3, believed to act as a sort of hinge (22); and adenosines in J4/5 and J5/4, which were proposed to interact with 2'-hydroxyl groups in the upper part of the P1 stem (18). In addition, several other changes in the reactivity pattern were observed, nearly all of which can be accounted for by disruption of previously proposed tertiary interactions (23).

The fact that all of the inhibitory drugs gave essentially identical footprints, in spite of their different structures and different inhibitory concentrations, is unexpected and could be interpreted as evidence for a single binding site. This is reinforced by the preliminary finding that all of the antibiotic-dependent protections and enhancements appear to have a similar dependence on drug concentration (19). However, it could also be argued that group I introns have multiple antibiotic binding sites and that their specificities for the different drugs and affinities for the multiple sites are coincidentally similar. In support of this interpretation is the finding that aminoglycoside antibiotics inhibit group I introns with mutated G-binding sites at the same concentration as that required for inhibition of the wild-type intron. If the protected G residue in the cofactor binding site were a contributor to the binding interaction of the antibiotic, then these mutations would be expected to weaken the interaction, leading to a requirement for significantly higher drug concentrations to cause inhibition. Multiple binding sites would also account for the mixed competitive-noncompetitive mode of inhibition observed for the neomycin-related drugs (12). Here it could be imagined that binding to the cofactor binding site would cause competitive inhibition, whereas binding to a second site, and therefore preventing P1 stem from binding to the J8/7 region, would cause noncompetitive inhibition.

The inhibition of two apparently unrelated functions of RNA splicing and translation by the same group of antibiotics is an unexpected finding. It will therefore be of interest to see whether there is an underlying similarity between the molecular mechanisms of action of 16S ribosomal RNA (rRNA) and group I introns. Schroeder has



**Fig. 5.** Inhibition of splicing by 5-epi-sisomicin in an intron containing a mutated cofactor binding site. Wild-type or mutant (G264-C311 to C264-G311) *Tetrahymena* intron RNA (6) was incubated under splicing conditions (31) with the appropriate cofactor (guanosine for the wild type, purine riboside for the mutant) in the presence or absence of 5-epi-sisomicin at the indicated concentrations (given in micromolar). WT, wild-type intron; G, guanosine; rP, purine riboside; Circ. intron, circular intron; Lig. exons, ligated exons; I. intron, linear intron.

recently suggested a structural analogy between the two systems (14). Splicing and decoding both involve recognition of a short helix of variable sequence by a conserved functional domain. In the case of splicing, this consists of interaction of the variable 5' splice site helix (P1) with the conserved catalytic core, in particular with the J8/7 sequence. In the ribosomal decoding site, the codon-anticodon helix, also variable in sequence, interacts with the conserved 1400 and 1500 regions of 16S rRNA (24). This similarity can be extended to the patterns of aminoglycoside protection observed for 16S rRNA and the group I intron; in both cases, binding of aminoglycosides results in protection of two guanine nucleotides at their N-7 positions and a single adenine at N-1 (25, 26). Whether these analogies correspond to structural homologies is presently unclear. If this turns out to be the case, it will serve to focus attention on the question as to whether these two functional RNAs have a common evolutionary origin.

#### REFERENCES AND NOTES

1. T. R. Cech, *Annu. Rev. Biochem.* **59**, 543 (1990).
2. F. Michel, A. Jaquier, B. Dujon, *Biochimie* **65**, 867 (1982); R. W. Davies, R. B. Waring, J. A. Ray, T. A. Brown, C. Scazzocchio, *Nature* **300**, 719 (1982).
3. For numbering of bases, the first base of the intron was labeled 1, therefore the guanine in the guanosine binding site was labeled G96. Stem (P<sub>n</sub>, n = 1, 2, ..., 9), loop (Ln), and single-stranded junction (J<sub>n/m</sub>) region numbering can be compared in Fig. 3.

4. F. Michel, P. M. Hanna, R. Green, D. P. Bartel, J. W. Szostak, *Nature* **342**, 391 (1989).
5. T. Inoue, F. X. Sullivan, T. R. Cech, *J. Mol. Biol.* **189**, 143 (1986).
6. M. D. Been and A. Perrotta, *Science* **252**, 434 (1991).
7. B. Bass and T. R. Cech, *Biochemistry* **25**, 4473 (1986).
8. M. Yarus, *Science* **240**, 1751 (1988).
9. U. von Ahsen and R. Schroeder, *Nature* **346**, 801 (1990).
10. ———, *Nucleic Acids Res.* **19**, 2261 (1991).
11. U. von Ahsen, J. Davies, R. Schroeder, *Nature* **353**, 368 (1991).
12. ———, *J. Mol. Biol.* **226**, 935 (1992).
13. H. F. Noller, *Nature* **353**, 302 (1991).
14. J. Davies, U. von Ahsen, R. Schroeder, in *The RNA World* (Cold Spring Harbor Laboratory Press, Cold Spring Harbor, NY, in press).
15. M. Q. Xu and D. A. Shub, *Gene* **87**, 77 (1989). In this study, we used the same sunY clone with the deletion in L9.1 as in (12).
16. S. Stern, D. Moazed, H. F. Noller, *Methods Enzymol.* **164**, 481 (1988). We assessed the accessibility of specific atoms on individual bases by monitoring the reactivity of adenine at N-1, cytosine at N-3, and guanine at N-7 toward DMS; guanine at N-1 and N-2 toward ketoxal; and uracil at N-3 toward 1-cyclohexyl-3-(2-morpholinoethyl)carbodiimide metho-*p*-toluene sulfonate.
17. T. Inoue and T. R. Cech, *Proc. Natl. Acad. Sci. U.S.A.* **82**, 648 (1985); J. A. Jaeger, M. Zuker, D. H. Turner, *Biochemistry* **29**, 10147 (1990).
18. F. Michel and E. Westhof, *J. Mol. Biol.* **216**, 585 (1990).
19. U. von Ahsen and H. F. Noller, unpublished results.
20. A. M. Pyle, F. L. Murphy, T. R. Cech, *Nature* **358**, 123 (1992).
21. Ligand-dependent protection from chemical attack can be due to indirect as well as direct interactions between the ligand and the protected site or by blocking access of reagent to the site.
22. B. Young, D. Herschlag, T. R. Cech, *Cell* **67**, 1007 (1991); D. Herschlag, *Biochemistry* **31**, 1386 (1992).
23. F. Michel, A. D. Ellington, S. Couture, J. W. Szostack, *Nature* **347**, 578 (1990). By inspecting the three-dimensional model of the *Tetrahymena* rRNA intron as well as the sunY intron (18, 27), we detected that nucleotide A70 (J6/6a-4) is in close vicinity to G144 (P3'-5), another nucleotide that shows chemical reactivity change in the presence of the drug.
24. D. Moazed and H. F. Noller, *Cell* **47**, 985 (1986); *J. Mol. Biol.* **211**, 135 (1990).
25. ———, *Nature* **327**, 389 (1987).
26. J. Woodcock *et al.*, *EMBO J.* **10**, 3099 (1991).
27. F. Michel *et al.*, *Genes Dev.* **6**, 1373 (1992).
28. D. A. Peattie, *Proc. Natl. Acad. Sci. U.S.A.* **76**, 1760 (1979).
29. In vitro-transcribed and gel-purified sunY precursor RNA (12) was renatured as described previously (27) and incubated for 15 min at 37°C in 80 mM potassium cacodylate (pH 7.2), 4 mM MgCl<sub>2</sub>, 50 mM NH<sub>4</sub>Cl with 50 μM neomycin B, 50 μM 5-epi-sisomicin, 50 μM kanamycin A, or 500 μM streptomycin (5-epi-sisomicin was provided by J. Davies; all other antibiotics were purchased from Sigma). RNA (1 to 5 pmol) was probed in a 50-μl reaction volume. For DMS reaction, 1 μl of 1:20 (in ethyl alcohol) diluted DMS was added and incubated at 37°C for 10 min. After incubation the reactions were stopped, 10 μg of tRNA as carrier were added and then precipitated, and primer extensions using α-<sup>32</sup>P-labeled deoxythymidine triphosphate to label cDNA were done as described (16). For detection of N-7 positions of guanosine nucleosides, an aniline-induced strand scission was performed (28). Products were separated on a 6% polyacrylamide gel.
30. 3'-Deoxyguanosine was purified by high-performance liquid chromatography on a Synchropak RPP 25-cm reversed-phase column to eliminate guanosine contamination. A linear gradient of 15 mM ammonium acetate in water to 30% acetonitrile

trile (including 15 mM ammonium acetate) in 60 min was carried out at a flow rate of 1 ml/min.

31. <sup>35</sup>S-labeled RNA derived from *Tetrahymena* rRNA wild-type intron (pBFSN-1) and mutant G264: C311G:G414A [(6); the wild-type and mutant introns were provided by M. D. Been] were prepared as described (12). The wild-type or the mutant intron RNA was incubated for 15 min at 37°C under splicing conditions [40 mM tris-HCl (pH 7.4), 10 mM MgCl<sub>2</sub>, 200 mM NaCl, 0.4 mM spermidine]. Cofactors were used at their concentrations (6) as follows: guanosine, 10 μM, and purine riboside, 300 μM (both from Sigma).

32. We thank R. Schroeder for discussions and comments and our colleagues in the Noller Laboratory for advice on experimental methods and for useful discussions. E. Westhof provided helpful information in explaining the perturbations in terms of the three-dimensional model for the group I intron. This research was sponsored by a long-term fellowship from the European Molecular Biology Organization (U.v.A.), NIH grant GM17129 (H.F.N.), and a grant to the CMB/RNA from the Lucille P. Markey Charitable Trust.

22 December 1992; accepted 10 March 1993

## New Domain Motif: The Structure of Pectate Lyase C, a Secreted Plant Virulence Factor

Marilyn D. Yoder, Noel T. Keen, Frances Journak\*

Pectate lyases are secreted by pathogens and initiate soft-rot diseases in plants by cleaving polygalacturonate, a major component of the plant cell wall. The three-dimensional structure of pectate lyase C from *Erwinia chrysanthemi* has been solved and refined to a resolution of 2.2 angstroms. The enzyme folds into a unique motif of parallel β strands coiled into a large helix. Within the core, the amino acids form linear stacks and include a novel asparagine ladder. The sequence similarities that pectate lyases share with pectin lyases, pollen and style proteins, and tubulins suggest that the parallel β helix motif may occur in a broad spectrum of proteins.

Pectate lyases (E.C. 4.2.2.2) are microbial extracellular enzymes that are important during plant pathogenesis (1). The enzymes randomly cleave α-1,4 linked galacturonosyl residues of the pectate component found in the primary cell wall and intercellular regions of higher plants. Enzymatic cleavage of the glycosidic bond occurs at a pH optimum of 8 to 11 through a β elimination mechanism, resulting in an unsaturated C-4-C-5 bond in the galacturonosyl moiety at the nonreducing end of the polysaccharide (1). Calcium is essential for enzymatic activity, but it is unclear whether Ca<sup>2+</sup> binds to the protein or to the substrate (2). Pectate lyases usually exist as multiple, independently regulated isozymes that are 27 to 80% identical in amino acid sequence (3, 4).

Pectate lyase C (PelC) was isolated from the periplasm of *Escherichia coli* cells containing a high-expression plasmid construct of the *pelC* gene from *Erwinia chrysanthemi* EC16 (5, 6). The periplasmic form of recombinant PelC has the identical molecular weight, isoelectric point, and maceration properties as the *E. chrysanthemi* isolate (7). The enzyme has 353 amino acids and a molecular weight of 37,676 (6). Crystals of PelC were grown from ammonium sulfate and belong to space group *P2<sub>1</sub>2<sub>1</sub>2<sub>1</sub>* with

unit-cell parameters of  $a = 73.38 \text{ \AA}$ ,  $b = 80.26 \text{ \AA}$ , and  $c = 95.12 \text{ \AA}$  and one molecule per asymmetric unit (8). The structure was solved with multiple isomorphous replacement (MIR) techniques (9). The model, which includes the first 352 residues but no solvent, has a crystallographic refinement factor of 20.2% for all measured reflections with structure-factor amplitude

$F > 2\sigma$  in the 2.2 to 5.0 Å resolution shell. The root-mean-square deviations are 0.006 Å from bond length ideality and 1.38° from bond angle ideality.

Because the structural motif of PelC is unusual, the correctness of the model was of particular concern throughout the analysis. In the initial stages of interpretation, there were few ambiguous regions in either the polypeptide tracing or in the amino acid sequence assignment in the MIR electron density maps. Furthermore, all heavy atom derivatives substituted at chemically reasonable sites: platinum at Met<sup>26</sup>, osmium at His<sup>153</sup>, and uranyl and lead at a common site in a pocket formed by Asp<sup>131</sup>, Glu<sup>166</sup>, and Asp<sup>170</sup>. After refinement, all carbonyl oxygens were visible in the final  $2F_0 - F_c$  electron density map (Fig. 1). All connections and polypeptide directions found in  $2F_0 - F_c$  maps, in which 10% of the total residues were sequentially omitted from the model, were consistent with those of the refined model. Only three residues were outside the normal range of the φ and ψ angles for standard secondary structural elements (Fig. 2A). Two additional measures supported the validity of the model (Fig. 2B).

The polypeptide backbone of PelC folds into a single structural domain (Fig. 3). The predominant secondary structural elements are parallel β strands that are coiled into a large right-handed cylinder that we call a parallel β helix. The NH<sub>2</sub>-terminal end of the cylinder is covered by a short α helix of three turns, and the COOH-terminal end is covered by polypeptide loops. Polypeptide loops also protrude from the

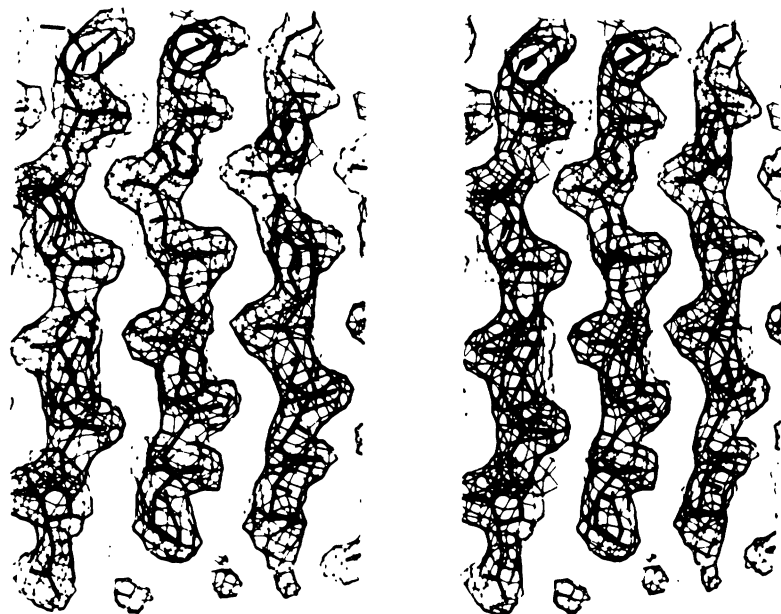


Fig. 1. Stereo view of the superposition of the backbone of several parallel β strands on the final  $2F_0 - F_c$  electron density map of PelC contoured at  $1.0 \sigma$ . The model is shown in black lines, and the electron density map is in gray lines. All carbonyl oxygen atoms are apparent in the final map.

M. D. Yoder and F. Journak, Department of Biochemistry, University of California, Riverside, CA 92521.  
N. T. Keen, Department of Plant Pathology, University of California, Riverside, CA 92521.

\*To whom correspondence should be addressed.